

# Metabolically induced NASH in obese LDLr<sup>-/-</sup>.Leiden mice share common molecular responses with NASH patients

**Arienne van Koppen<sup>2</sup>**  
**Reinout Stoop<sup>2</sup>**  
**Roeland Hanemaaijer<sup>2</sup>**  
**Martien Caspers<sup>1</sup>**  
**Martine Morrison<sup>2</sup>**  
**Kanita Salic<sup>2</sup>**  
**Anita van den Hoek<sup>2</sup>**  
**Robert Kleemann<sup>2</sup>**  
**Lars Verschuren<sup>1#</sup>**

<sup>1</sup> TNO Microbiology and Systems Biology  
<sup>2</sup> TNO Metabolic Health Research

# Lars.Verschuren@tno.nl

**TNO** innovation for life

## Introduction

Mouse models of NAFLD are the cornerstone for mechanistic studies of disease pathogenesis and frequently used for the screening of pharmacological interventions. However, not all models represent human pathology and etiology to a similar extent. One way to define predictability of these mouse models is to compare their molecular response involved in disease development with those present in NASH.

## Methods

We analyzed the time-resolved molecular responses in two different diet-induced mouse models of NAFLD/NASH/fibrosis (High Fat Diet (HFD)-fed LDLr<sup>-/-</sup>.Leiden mice and High Fat and Cholesterol (HFC)-fed ApoE3Leiden\* CETP mice). Human gene expression dataset was used as published by Ahrens M, 2013 and originates from Gene Expression Omnibus (GSE48452). Differentially expressed genes as compared to their study-controls were used as input for comparison between mice and men. Analysis was performed on single gene and pathway level using bioinformatics tools.

species	regulated genes (mapped)	HO	NAFLD	NASH	HF12	HF18	STZ12	STZ18	MCD4	MCD8	Pten	HF30	WTD	species
HO	12 (10)	0	1	0	0	0	0	0	0	0	0	0	0	HO
NAFLD	65 (51)	7	0	34	6	4	4	2	0	2	0	0	15	NAFLD
NASH	177 (123)	9	47	0	5	2	4	1	0	3	0	0	24	NASH
HF12	149 (126)	0	1	3	0	3	13	3	13	7	0	0	5	HF12
HF18	35 (28)	0	1	2	9	3	4	24	2	2	0	12	11	HF18
STZ12	55 (35)	1	1	3	26	11	3	3	1	1	0	6	6	STZ12
STZ18	71 (57)	0	1	2	22	25	25	2	2	2	0	12	8	STZ18
MCD4	703 (573)	0	4	10	38	6	17	21	11	1	3	4	4	MCD4
MCD8	1098 (909)	0	4	18	41	12	22	35	572	0	4	3	3	MCD8
Pten	91 (75)	1	3	3	7	5	3	7	8	9	0	1	1	Pten
HF30	236 (206)	0	1	6	11	16	11	29	62	91	10	9	9	HF30
WTD	125 (108)	0	1	3	21	8	17	15	44	44	11	31	31	WTD

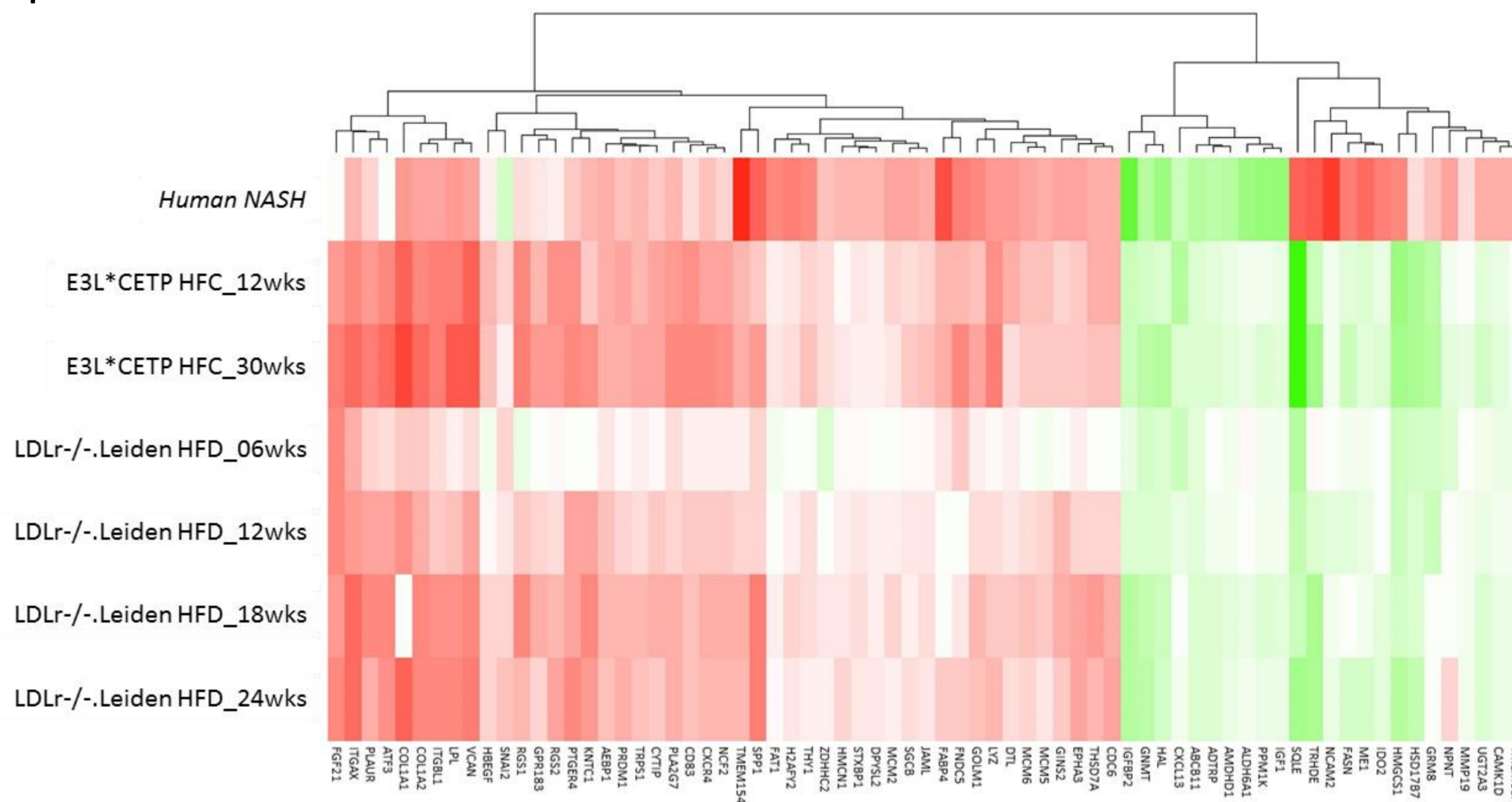
Table 1. the dataset GSE48452 was used recently (Teufel et al, 2016) and demonstrate very little overlap of genes in human NASH as compared to mouse models.

## Conclusions:

- Analysis of individual genes demonstrate that a large part of the human regulated genes are represented in two diet-induced mouse models.
- Enrichment analysis of biological processes demonstrate overlap between mouse and men in processes related to LXR-activation, inflammation and hepatic stellate cell activation.
- 66% of the canonical pathways in human are represented in the mouse models. Among them lipid metabolism, inflammation and hepatic fibrosis.

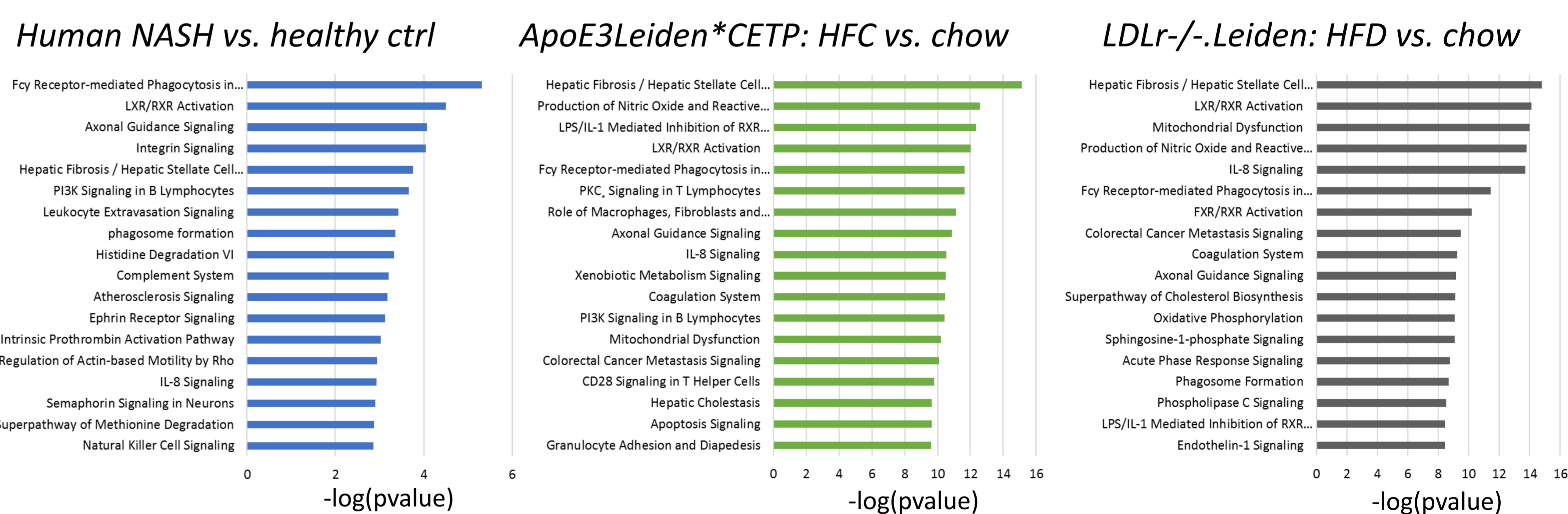
## Results:

Overlap of pre-selected individual genes (as documented by Teufel et al.) in human NASH patients and mouse models for NASH.



These data demonstrate that 71 genes with distinct expression pattern (green is downregulated, red is upregulated) in human NASH biopsies have significant overlap with expression in both mouse models.

Comparison of top-18 significant pathways after enrichment analysis of differently expressed genes in both human NASH and mouse models



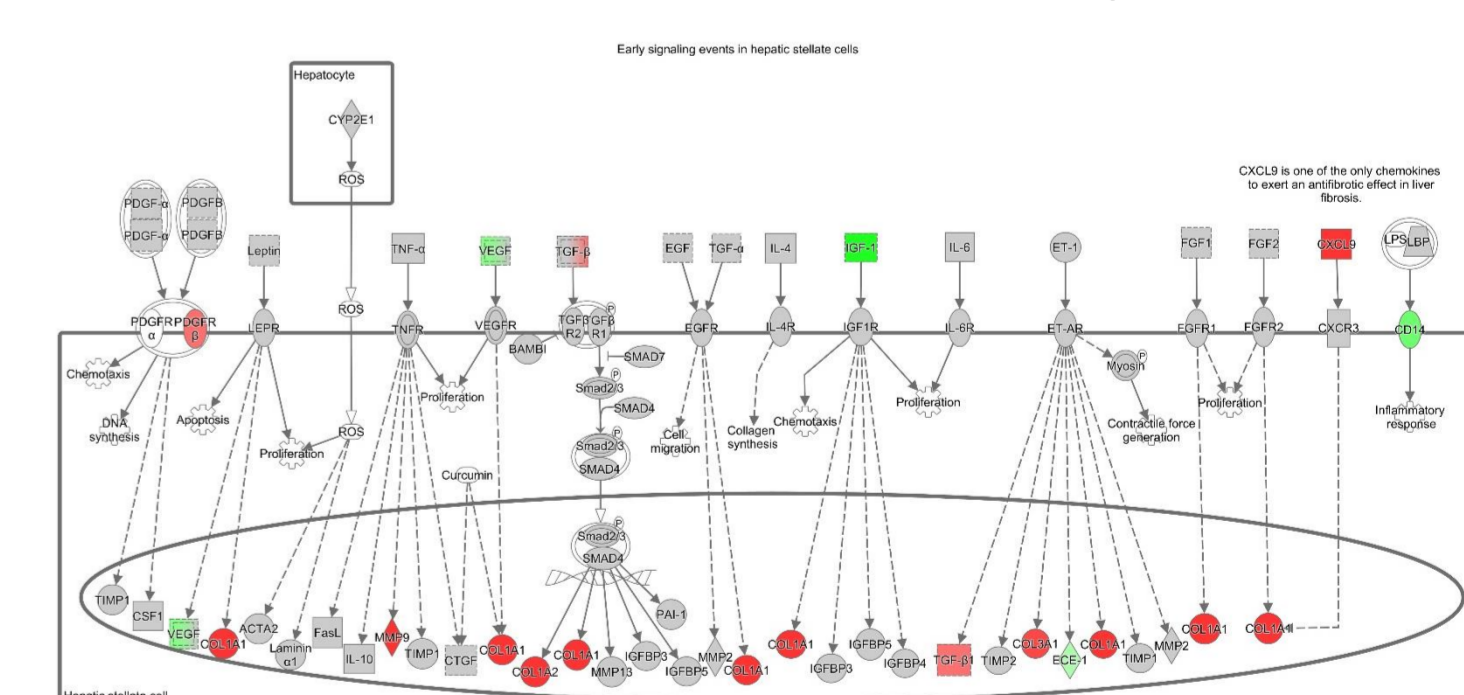
These data demonstrate overlap between human and mouse models in the biological processes LXR-activation, inflammation and hepatic stellate cell activation.

The 29 significantly differentially expressed canonical pathways for human NASH and their significance in mouse

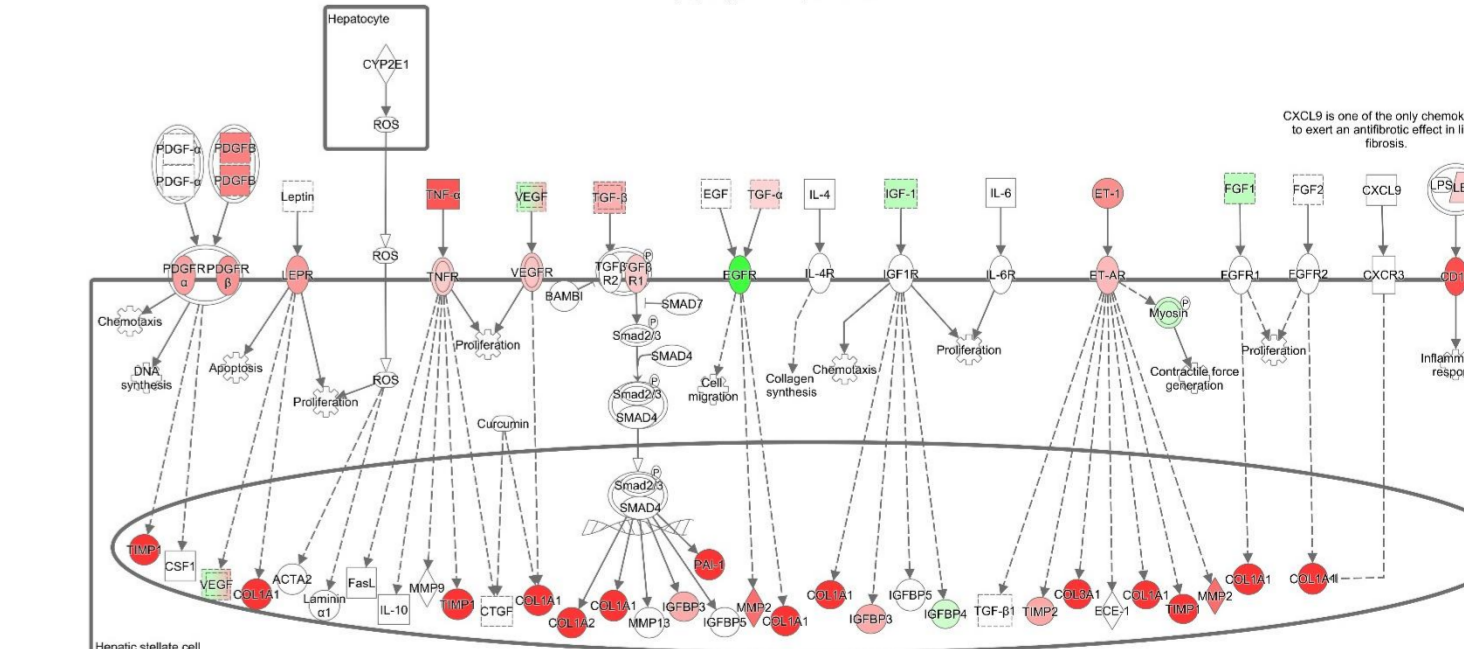
Pathway Analysis (IPA)	Significant in Mouse = Red: 66% of Significant Human Pathways
The 29 Significant Human Canonical Pathways (-log <sub>10</sub> p>2)	ApoE3 Leiden * CETP
Hepatic Fibrosis / Hepatic Stellate Cell Activation	Red
LXR/RXR Activation	Red
Fcγ Receptor-mediated Phagocytosis in Macrophages	Red
Coagulation System	Red
PI3K Signaling in B Lymphocytes	Red
Acute Phase Response Signaling	Red
FXR/RXR Activation	Red
Superpathway of Cholesterol Biosynthesis	Red
Extrinsic Prothrombin Activation Pathway	Red
Dendritic Cell Maturation	Red
Caveolar-mediated Endocytosis Signaling	Red
Intrinsic Prothrombin Activation Pathway	Red
Cholesterol Biosynthesis I	Red
Cholesterol Biosynthesis II (via 24,25-dihydrolanosterol)	Red
Cholesterol Biosynthesis III (via Desmosterol)	Red
Zymosterol Biosynthesis	Red
mTOR Signaling	Red
Histidine Degradation III	Red
Superpathway of Methionine Degradation	Red
Superpathway of Inositol Phosphate Compounds	Red
Histidine Degradation VI	Red
Complement System	Red
Oleate Biosynthesis II (Animals)	Red
Fatty Acid Biosynthesis Initiation II	Red
Palmitate Biosynthesis I (Animals)	Red
Epoxyqualene Biosynthesis	Red
β-alanine Degradation I	Red
Cell Cycle Control of Chromosomal Replication	Red
EIF2 Signaling	Red

66% of the human pathways also show significant differential expression in the mouse models (ApoE3Leiden\*CETP and LDLr<sup>-/-</sup>.Leiden). Among them are the most important NASH related biological processes: lipid metabolism, inflammation and hepatic stellate cell activation (see figure on the right).

### Human NASH vs. healthy controls



### ApoE3Leiden\*CETP: HFC vs. chow



### LDLr<sup>-/-</sup>.Leiden: HFD vs. chow

